

## Free-standing versus AIAs-embedded GaAs quantum dots, wires, and films: The emergence of a zero-confinement state

Alberto Franceschetti and Alex Zunger

Citation: [Applied Physics Letters](#) **68**, 3455 (1996); doi: 10.1063/1.115791

View online: <http://dx.doi.org/10.1063/1.115791>

View Table of Contents: <http://scitation.aip.org/content/aip/journal/apl/68/24?ver=pdfcov>

Published by the [AIP Publishing](#)

---

### Articles you may be interested in

[Photoluminescence studies of self-assembled InSb, GaSb, and AlSb quantum dot heterostructures](#)  
Appl. Phys. Lett. **68**, 3614 (1996); 10.1063/1.115747

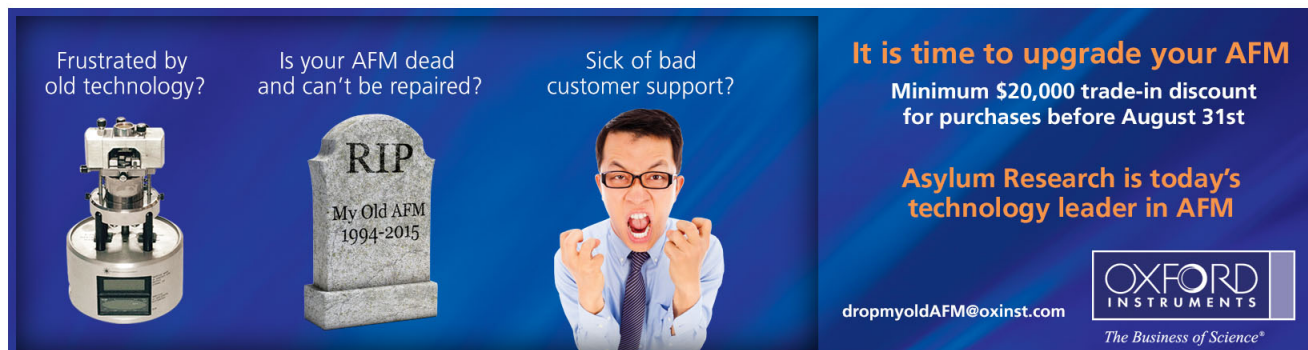
[Stresses and strains in lattice-mismatched stripes, quantum wires, quantum dots, and substrates in Si technology](#)  
J. Appl. Phys. **79**, 8145 (1996); 10.1063/1.362678

[Strain and quantum confinement energies in n-type modulation-doped lattice-mismatched InAsP quantum-well wires](#)  
J. Appl. Phys. **79**, 8456 (1996); 10.1063/1.362521

[InGaAs/GaAs quantum wires and dots defined by low-voltage electron-beam lithography](#)  
J. Vac. Sci. Technol. B **13**, 2888 (1995); 10.1116/1.588311

[Fabrication of CdZnSe/ZnSe quantum dots and quantum wires by electron beam lithography and wet chemical etching](#)  
J. Vac. Sci. Technol. B **13**, 2792 (1995); 10.1116/1.588267

---

An advertisement for Oxford Instruments' AFM technology. The background is dark blue with a subtle light pattern. On the left, there is an image of a white AFM instrument. In the center, a man in a blue shirt and tie is shown with a frustrated expression, shouting with his hands raised. To his left is a grey tombstone with the inscription 'RIP My Old AFM 1994-2015'. Text on the left side asks: 'Frustrated by old technology?', 'Is your AFM dead and can't be repaired?', and 'Sick of bad customer support?'. On the right side, the text reads: 'It is time to upgrade your AFM', 'Minimum \$20,000 trade-in discount for purchases before August 31st', and 'Asylum Research is today's technology leader in AFM'. At the bottom right, the Oxford Instruments logo is shown with the tagline 'The Business of Science®' and the email address 'dropmyoldAFM@oxinst.com'.

# Free-standing versus AlAs-embedded GaAs quantum dots, wires, and films: The emergence of a zero-confinement state

Alberto Franceschetti and Alex Zunger  
National Renewable Energy Laboratory, Golden, Colorado 80401

(Received 26 January 1996; accepted for publication 5 April 1996)

Using a plane-wave pseudopotential method we investigate the electronic structure of free-standing and of AlAs-embedded GaAs quantum dots, wires, and films. We predict that (i) the confinement energy of the valence-band maximum (VBM) is larger in AlAs-embedded than in free-standing quantum structures, because of the zero-confinement character of the VBM wave function in the latter case; (ii) small GaAs quantum structures have an indirect band gap, whereas large GaAs quantum structures have a direct band gap; (iii) the conduction-band minimum of small free-standing quantum structures originates from the GaAs  $X_{1c}$  valley, while it derives from the AlAs  $X_{1c}$  state in AlAs-embedded quantum structures; (iv) the critical size for the direct/indirect crossover is larger in embedded quantum structures than in free-standing quantum structures.

© 1996 American Institute of Physics. [S0003-6951(96)02124-9]

Semiconductor nanostructures have received great attention in recent years, both from an experimental and a theoretical point of view. Several techniques have been developed to confine carriers in two or three dimensions, leading to the realization of quantum wires and dots. The two general strategies commonly used to realize quantum confinement rely on (i) embedding the semiconductor quantum structure in a larger-gap semiconductor barrier (e.g. GaAs in AlGaAs or InGaAs in GaAs), or (ii) using an organic solvent to create a confining barrier for the semiconductor quantum structure. In the former case (embedded quantum structures), effective-mass based methods often provide a simple and sufficiently accurate model to predict and interpret the experimental results, while in the latter case (free-standing quantum structures) the agreement of such simple theoretical models with experiment is much worse.<sup>1</sup>

In this work, we contrast the electronic properties of (a) AlAs-embedded and (b) free-standing GaAs quantum films, wires and dots using a direct pseudopotential method. We find that, quite surprisingly, the confinement energy of the valence-band maximum (VBM) is larger in AlAs-embedded than in free-standing (hydrogen passivated) quantum structures, due to the “zero-confinement” character of the VBM in the latter case. This effect depends on the crystallographic orientation of the sample surfaces, but should otherwise be present in any zinc-blende free-standing quantum structure. We also find that *small* GaAs quantum structures always have an *indirect* band gap. In the case of free-standing quantum structures the conduction-band minimum (CBM) originates from the GaAs  $X_{1c}$  conduction state, thus making the quantum structure *intrinsically* indirect (type-I alignment in real space). In the case of AlAs-embedded quantum structures the CBM originates from the  $X_{1c}$  conduction state that is localized in the AlAs matrix, leading to a type-II alignment in real space. *Large* GaAs quantum structures, on the other hand, have a *direct* band gap, with the CBM originating from the GaAs  $\Gamma_{1c}$  state. Thus, for both free-standing and AlAs-embedded GaAs quantum structures we predict an indirect  $\rightarrow$  direct transition as the size increases; the critical

size for this transition is larger in AlAs-embedded than in free-standing quantum structures.

Rather than use the conventional effective-mass approximation or the eight-band  $\mathbf{k}\cdot\mathbf{p}$  model, we solve the single-particle Schrodinger equation for the quantum structure, using an atomistic, microscopic potential:

$$\left[ -\frac{1}{2}\nabla^2 + V(\mathbf{r}) \right] \psi_i(\mathbf{r}) = \epsilon_i \psi_i(\mathbf{r}). \quad (1)$$

The pseudopotential of the quantum structure,  $V(\mathbf{r})$ , is obtained as a superposition of screened atomic pseudopotentials,<sup>2</sup> fitted to measured interband transition energies, effective masses and deformation potentials of bulk GaAs and AlAs, and to calculated wave functions and level splittings of GaAs/AlAs short-period superlattices. The surface dangling bonds of free-standing GaAs quantum structures are passivated using hydrogen-like pseudopotentials,<sup>3</sup> in order to remove the surface states from the band gap. The quantum structure wave functions  $\psi_i(\mathbf{r})$  are expanded in a plane-wave basis set, including up to  $\sim 10^5$  basis functions. The band-edge energies and wave functions are obtained from Eq. (1) using the Folded Spectrum Method,<sup>4</sup> with a computational effort that scales only linearly with the size of the system.

We consider first (110)-oriented GaAs quantum films. The VBM and CBM energies at the center of the 2D Brillouin zone are shown in Fig. 1(a) as a function of the film thickness  $L$  (note that in the  $\langle 110 \rangle$  directions 1 GaAs ML  $\approx 2.0$  Å). The shaded region indicates the GaAs *bulk* band gap. Remarkably, we see that in the case of free-standing, hydrogen-passivated quantum films (dashed lines) the VBM energy is almost thickness independent, and is nearly degenerate with the bulk GaAs  $\Gamma_{15v}$  energy. We refer to this property as “zero confinement”: the VBM energy is insensitive to quantum confinement effects. In the language of the effective-mass approximation, the quantum-structure wave function is represented as the product of a Bloch-periodic wave function times a slowly varying, sine-like envelope function, which satisfies the boundary conditions. An analysis of the calculated VBM wave function (Fig. 2) shows in-

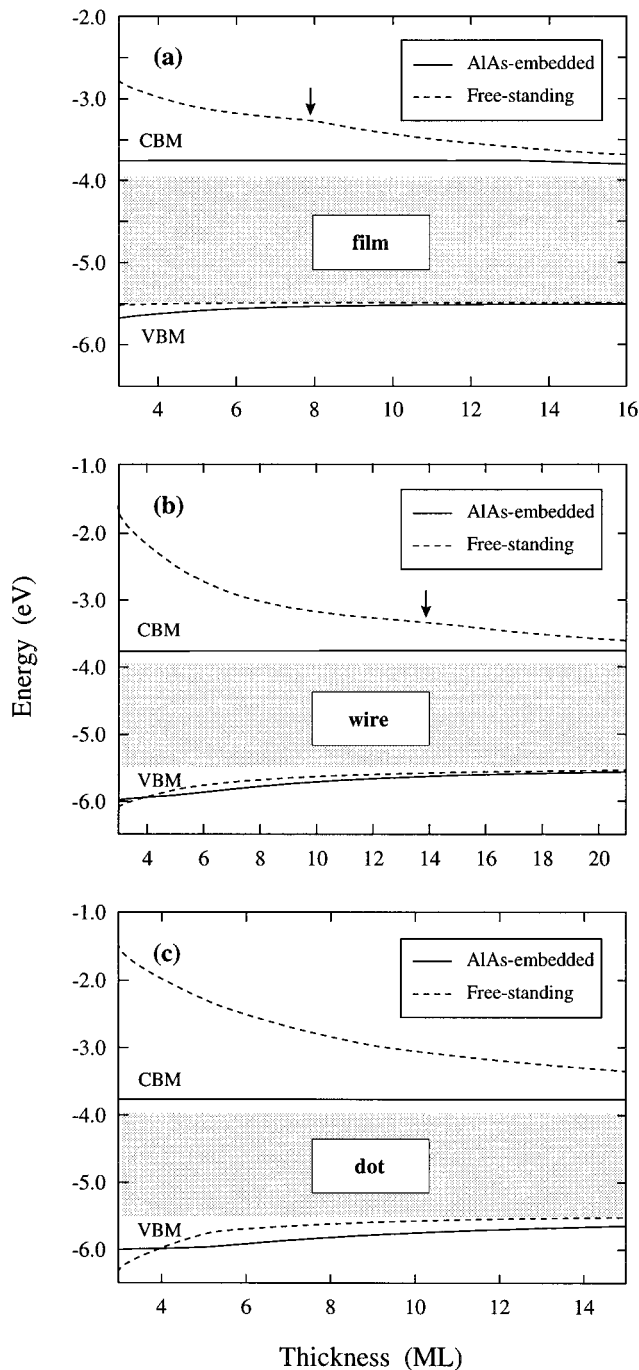


FIG. 1. Band-edge energies of AlAs-embedded (solid lines) and free-standing (dashed lines) GaAs quantum films (a), wires (b), and dots (c). The shaded areas denote the GaAs bulk band gap. The arrows indicate the critical size for the direct/indirect transition in free-standing quantum films and wires.

stead that the VBM envelope function is almost constant for  $(1\bar{1}0)$  quantum films, and that the  $\Gamma_{15v}$  Bloch-periodic wave function nearly vanishes at the boundary of the quantum film, automatically satisfying zero boundary conditions. In the case of AlAs-embedded films the VBM energy *does* depend on the film thickness, and the VBM envelope function has the usual sine-like form predicted by the effective-mass approximation (Fig. 2), thus explaining the larger confinement energy of the VBM state.

A wave-function analysis shows that the CBM of free-

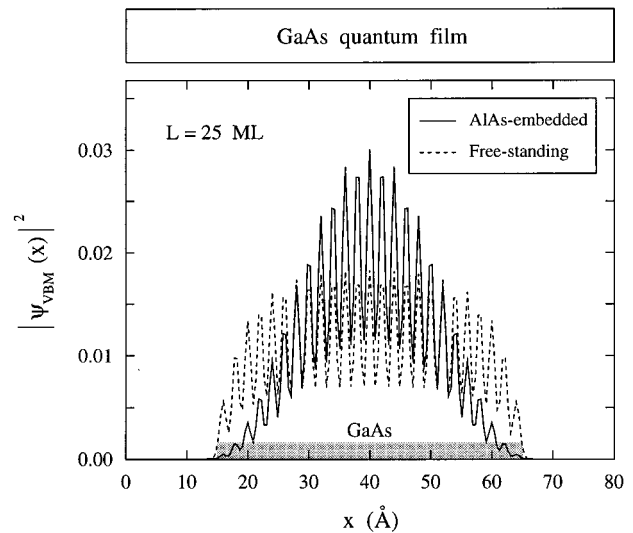


FIG. 2. VBM wavefunction amplitude of AlAs-embedded (solid line) and free-standing (dashed line) GaAs  $(1\bar{1}0)$  quantum films of thickness  $L = 25$  ML = 50 Å. The wave-function amplitude, averaged over the  $(110)$  planes, is plotted along the  $[1\bar{1}0]$  direction.

standing GaAs quantum films originates from the bulk  $X_{1c}^z$  valley for  $L < 8$  ML, while it becomes a  $\Gamma_{1c}$ -derived state for  $L > 8$  ML (see also Table I). The direct/indirect crossover is evident in Fig. 1(a) as a kink of the energy vs thickness curve at  $L \sim 8$  ML. In AlAs-embedded thin films, on the other hand, quantum-confinement effects push the  $\Gamma$ -like conduction-band state of GaAs above the  $X$ -like conduction-band minimum of AlAs, exposing the latter as the CBM, as discussed in Ref. 5. Thus, the CBM energy of AlAs-embedded thin films ( $L < 13$  ML) is pinned at the bulk AlAs  $X_{1c}$  value, and the CBM wave function is localized in the AlAs region, giving origin to a type-II alignment in real space. For thicker films ( $L > 13$  ML) the CBM becomes a  $\Gamma$ -like state localized in the GaAs film, leading to a type-I alignment in real space. Thus, the indirect  $\rightarrow$  direct transition in AlAs-embedded quantum films corresponds to a type II  $\rightarrow$  type-I transition in real space. The VBM and CBM wave functions of free-standing and AlAs-embedded indirect-gap quantum films ( $L = 7$  ML) are compared in Fig. 3; the different spatial localization of the CBM wave functions and the ensuing different alignment in real space are evident in this figure.

We consider next GaAs quantum wires with square cross section; the surface planes are oriented in the  $(1\bar{1}0)$  and  $(110)$  directions, and the wires are periodic in the  $[001]$  direction. The band-edge energies of free-standing and AlAs-embedded quantum wires (calculated at the zone center of the 1D Brillouin zone) are compared in Fig. 1(b) as a function of the wire size  $L$ . In this case the zero-confinement nature of the VBM state is only partial, as suggested by the

TABLE I. Critical sizes (in ML) for the direct/indirect crossover in free-standing and AlAs-embedded GaAs quantum films, wires, and dots.

	Film	Wire	Dot
Free-standing	8	14	> 15
AlAs-embedded	13	25	> 15

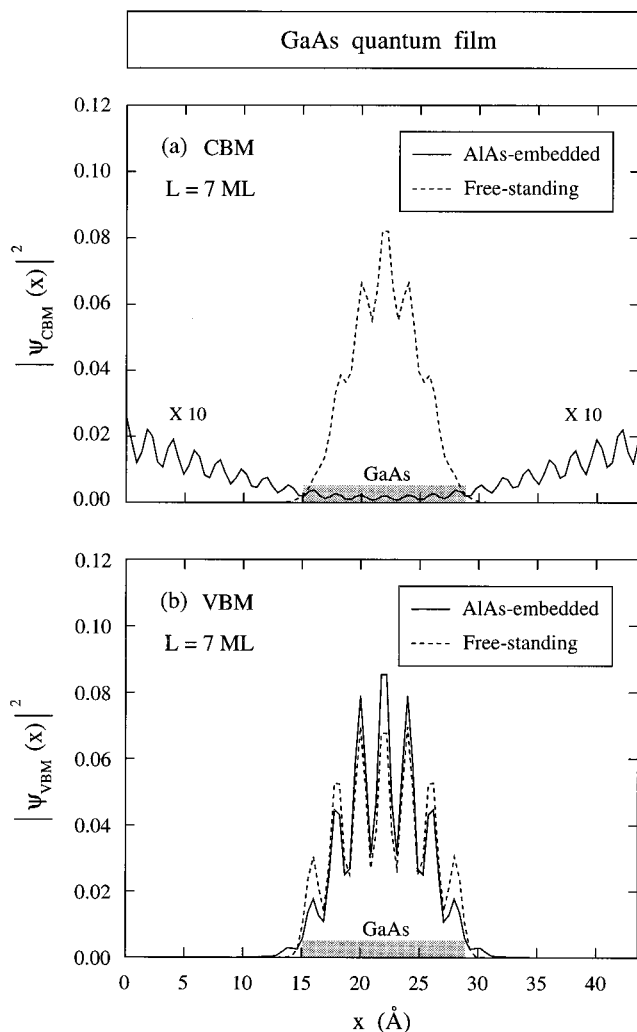


FIG. 3. (a) CBM and (b) VBM wave-function amplitude of AlAs-embedded (solid lines) and free-standing (dashed lines) GaAs  $(\bar{1}\bar{1}0)$  quantum films of thickness  $L=7$  ML= $14$  Å. The wave-function amplitude, averaged over the  $(\bar{1}\bar{1}0)$  planes, is plotted along the  $[\bar{1}\bar{1}0]$  direction. The CBM wave function of the AlAs-embedded film is normalized over a larger unit cell than the one shown in the figure. Note that the free-standing film is type-I, while the AlAs-embedded film is type-II.

size dependence of the VBM energy. Nevertheless, the VBM confinement energy of AlAs-embedded wires is still slightly larger than the VBM confinement energy of free-standing wires (for  $L \geq 5$  ML). The CBM of free-standing quantum wires originates from the GaAs  $X_{1c}$  valleys for thicknesses

up to  $L=14$  ML ( $28$  Å), while it becomes a  $\Gamma_{1c}$ -derived state for larger quantum wires (see also Table I). The CBM of AlAs-embedded quantum wires is an AlAs  $X_{1c}$ -derived state in all the size range considered here; it is predicted to become a GaAs  $\Gamma$ -derived state at the critical size  $L \sim 25$  ML ( $50$  Å), where the type-II  $\rightarrow$  type-I transition occurs.

Finally, we consider rectangular GaAs quantum boxes elongated in the  $[001]$  direction. The surface planes are oriented in the  $(\bar{1}\bar{1}0)$ ,  $(110)$ , and  $(001)$  directions. We have  $L_{1\bar{1}0}=L_{110}=L$  and  $L_{001}=\sqrt{2}L$ . The band-edge energies of free-standing and AlAs-embedded quantum boxes are compared in Fig. 1(c) as a function of the box size  $L$ . The VBM confinement energy is slightly larger in AlAs-embedded than in free-standing quantum dots (for  $L \geq 5$  ML). Unlike the case of quantum wires, however, the energy vs thickness curve of small AlAs-embedded quantum boxes has a positive (upward) curvature. This is due to the fact that a small GaAs dot embedded in AlAs cannot bind a hole. Thus, the VBM energy of the smallest GaAs quantum dot considered here ( $L=3$  ML) coincide with the VBM energy of bulk AlAs, and the corresponding wave function shows only a *resonance* on the GaAs quantum dot. The CBM of free-standing quantum boxes originates from the bulk GaAs  $X_{1c}$  valleys in all the size range considered here. The CBM of AlAs-embedded quantum boxes, on the other hand, is pinned at the energy of the bulk AlAs  $X_{1c}$  state, and the corresponding wave function is localized in the AlAs region.

In conclusion, using direct pseudopotential calculations we have shown that the VBM energy of free-standing GaAs quantum films, wires and dots is strongly affected by the zero-confinement character of this state, leading to a *smaller* confinement energy than in AlAs-embedded quantum structures. We have also demonstrated that quantum confinement effects can transform a direct-gap semiconductor such as GaAs into an indirect-gap system, with a mechanism similar to the well known pressure-induced  $\Gamma \rightarrow X$  transition in direct-gap semiconductors.

This work was supported by the U.S. Department of Energy, OER-BES, under Grant No. DE-AC36-83CH10093.

<sup>1</sup>See, for example, A. D. Yoffe, *Adv. Phys.* **42**, 173 (1993).

<sup>2</sup>K. A. Mäder and A. Zunger, *Phys. Rev. B* **50**, 17393 (1994).

<sup>3</sup>A. Franceschetti and A. Zunger, *J. Chem. Phys.* **104**, 5572 (1996).

<sup>4</sup>L. W. Wang and A. Zunger, *J. Chem. Phys.* **100**, 2394 (1994); *J. Phys. Chem.* **98**, 2158 (1994).

<sup>5</sup>A. Franceschetti and A. Zunger, *Phys. Rev. B* **52**, 14664 (1995).